INSTITUTE OF PHYSICS PUBLISHING NETWORK: COMPUTATION IN NEURAL SYSTEMS

Network: Comput. Neural Syst. **13** (2002) 195–216 PII: S0954-898X(02)35457-5

Complex dynamics and the structure of small neural networks

Frank Pasemann

Fraunhofer Institute for Autonomous Intelligent Systems, Schloss Birlinghoven, 53754 Sankt Augustin, Germany

E-mail: frank.pasemann@ais.fraunhofer.de

Received 31 August 2001
Published 30 April 2002
Online at stacks.iop.org/Network/13/195

Abstract

The discrete-time dynamics of small neural networks is studied empirically, with emphasis laid on non-trivial bifurcation scenarios. For particular two- and three-neuron networks interesting dynamical properties like periodic, quasi-periodic and chaotic attractors are observed, many of them co-existing for one and the same set of parameters. An appropriate equivalence class of networks is defined, describing them as parametrized dynamical systems with identical dynamical capacities. Combined symmetries in phase space and parameter space are shown to generate different representatives of such a class. Moreover, conditions on the connectivity structure are suggested, which guarantee the existence of complex dynamics for a considered equivalence class of network configurations.

(Some figures in this article are in colour only in the electronic version)

1. Introduction

For biological brains, anatomical as well as physiological observations indicate that neurons are grouped together into functional circuits, and certain small neural populations can be assumed to represent the basic building blocks of a modular organization of brains [1–4]. Although such hypothesized modules, like the hyper-columns [5], can be composed of as many as 10^5 neurons, already two-neuron circuits like the recurrent inhibitory loop [6–8] or three-neuron circuits, serving, for instance, as central pattern generators [9] are considered to represent the basic feedback mechanisms regulating neural activity in biological brains.

The widespread recurrent structures found in biological neural networks imply the possibility of complex neural dynamics and, in fact, oscillatory and chaotic activity has been observed frequently in brains [10–13]. This suggests that complex dynamics may play an important role for specific functions of the brain. Therefore, these dynamical properties have found increasing attention in recent years; but it still remains an open question to what extent

and through which kind of mechanisms oscillatory and chaotic dynamics can contribute to effective signal processing in the brain.

It seems obvious that artificial neural networks with higher information processing capabilities will also be built from a large collection of neurons, and a modular structure of these systems suggests itself. Following such a modular approach implies the attempt to understand the emergent dynamical properties of such a network in terms of interacting smaller subnetworks. Thus, it is considered as a rational first step to study small networks, called neuromodules in the following for obvious reasons, which already exhibit a complex dynamical behaviour. In various articles the dynamics of two- and three-neuron networks has been studied for different paradigms of artificial networks, for time-continuous systems as well as for the time-discrete case, for spiking neurons as well as for formal neurons [14–30]. Often the time-discrete dynamics of small recurrent networks has been investigated because their dynamics is easy to simulate, and their observed dynamical properties can be assumed to exist also in corresponding higher-dimensional time-continuous dynamical systems.

Of interest, therefore, are parameter domains, for which non-convergent dynamics of the neuromodules has to be expected; i.e. we are looking for domains for which there exist periodic or chaotic attractors. Thus, not only a fixed point analysis has to be done here, but the crucial data are obtained by the corresponding bifurcation sets in parameter space. A complete fixed point analysis for recurrent two-neuron networks has been given, for example, in [21] for the time-continuous case and in [30] for the time-discrete case.

This paper concentrates on the bifurcation structure of two- and three-neuron recurrent networks. They are composed of standard additive neurons having a strictly positive sigmoidal transfer function, and they will be considered as parametrized discrete-time dynamical systems. Relevant parameters are given by the strength of synaptic connections, the bias terms of neurons, and stationary or slowly varying external inputs, respectively. The connectivity structure of modules is assumed to satisfies Dale's rule; i.e. a given neuron has the same type of action at all its synapses, or otherwise stated, its outgoing connections are all either positive (excitatory) or negative (inhibitory). Correspondingly, a neuron is said to be excitatory or inhibitory. Although this rule is not always realized in biological networks, it will be used here as a simplifying paradigm for the organization of networks.

In the following studies emphasis is laid on chaotic dynamics, not because it is assumed that chaotic dynamics will play an essential role for functional neural processing, but because of the following fact: if a neural circuit allows parameter values, which lead to the observation of chaotic behaviour, then in general there exist parameter values for any kind of periodic behaviour (including, of course, also fixed point attractors). In this sense, these so-called *chaotic neuromodules* provide a large reservoir of dynamical properties. From this reservoir, a learning algorithm or convenient external driving signals may select those parameter values which lead, perhaps in cooperative interaction with other neuromodules of the system, to a desired or appropriate functional behaviour.

A second point which should be emphasized here, is the fact, that for fixed parameter values neuromodules can have different non-trivial attractors at the same time; for instance, a p-periodic attractor may co-exist with a chaotic attractor. Thus it depends on the initial conditions which asymptotic behaviour is finally observed. Co-existence of different attractors signifies multi-functionality of a module, and may lead to the observation of what has been called a *generalized hysteresis* phenomenon [24].

If a path of slowly varying parameters is crossing a bifurcation set, it depends on the direction of the path, leaving or entering the hysteresis domain, if there is a sudden jump in the qualitative behaviour of the system or not. A path in parameter space crossing the whole hysteresis domain in both directions will cause such jumps at different parameter

values, generating a *hysteresis loop* in state space. In the simplest case, referring to bistability of a system with two parameters, this phenomenon is associated with the so-called cusp catastrophe [31–33]. As shown in the following, already two-neuron networks have co-existing non-trivial attractors, like periodic attractors existing together with quasiperiodic or chaotic ones, and in three-neuron networks also co-existing chaotic attractors can be observed.

Finally, in respect of the neurodynamics approach to cognitive systems [34], we understand attractors only as classifying instruments. The dynamics of neural networks serving as embodied cognitive systems, for example as neuro-controllers acting in a sensori-motor loop, will always be that of a driven system. Of relevance for the behaviour of such biological or artificial embodied systems is only the structure of the basins of attraction in phase space. Or otherwise stated, what relates to a specific functional brain process are the transients in one and the same basin of attraction, not specific orbits in the state space of the system, especially not the attractor itself. Of course, the number, structure and size of basins, as well as their defining attractors, are controlled by the parameters of the neuromodules. Thus, different modes of behaviour may appear or disappear while crossing corresponding bifurcation sets.

The following section will give a short introduction to neurodynamics and sections 3 and 4 will illustrate these ideas with some simple examples of two- and three-neuron networks.

2. Discrete-time neurodynamics

In this section we will describe an n-neuron module, or *n-module* for short, as a parametrized family of n-dimensional discrete-time dynamical system $(\mathcal{A}, f_\rho)$ on an n-dimensional activity phase space $\mathcal{A} \subset \boldsymbol{R}^n$. With $\mathcal{Q} \subset \boldsymbol{R}^q$ denoting the q-dimensional parameter space, the dynamics is given by the map $f_\rho : \mathcal{A} \to \mathcal{A}$, $\rho \in \mathcal{Q}$, defined by

$$a_i(t+1) = \theta_i + \sum_{j=1}^{n} w_{ij}\,\sigma(a_j(t)), \qquad i = 1, \ldots, n. \tag{1}$$

Here a_i denotes the activity of unit i, w_{ij} denotes the synaptic weight from unit j to unit i, and $\theta_i = \overline{\theta}_i + I_i$ denotes the sum of its fixed bias term $\overline{\theta}_i$ and a stationary external input I_i. The output $o_i = \sigma(a_i)$ of the units is given by the strictly positive sigmoidal transfer function

$$\sigma(a) := \frac{1}{1+\mathrm{e}^{-a}}. \tag{2}$$

The parameter vector $\rho \in \mathcal{Q}$ has components $\theta_1, \ldots, \theta_n$ and $w_{11}, \ldots, w_{nn}$. The module dynamics (1) is always dissipative and bounded on an open domain $\mathcal{U} \subset \mathcal{A}$, with bounds given by

$$\theta_i - \sum_{j=1}^{n} |w_{ij}^-| < a_i < \theta_i + \sum_{j=1}^{n} w_{ij}^+, \tag{3}$$

where $w_{ij}^+ = w_{ij}$ if $w_{ij} > 0$, $w_{ij}^- = w_{ij}$ if $w_{ij} < 0$, and $w_{ij}^\pm = 0$ else.

As explained in the introduction we are mainly interested in network configurations for which complex dynamics has to be expected; i.e. we want to study parameter domains for which there exist interesting bifurcation scenarios like period-doubling routes to chaos, bifurcations from stable fixed points to higher-periodic or quasi-periodic attractors, and the like. To find such parameter domains is in general a difficult analytical task, and usually this will be done with the help of simulation techniques. A good starting point is to exclude all those parameter domains for which the system is convergent; i.e. it has only fixed point attractors. This is the case, for instance, for feedforward networks. But also networks with a symmetric (anti-symmetric) weight matrix will not be considered here, because they can have only fixed point

attractors and period-2 (period-4) attractors [35]. The convergence property of dynamical systems is often proven using its linearization. The linearization of an n-module $(\mathcal{A}, f_\rho)$ at a state $a^* \in \mathcal{A}$ is given by its Jacobian matrix Df_ρ, which reads

$$(Df_\rho)_{ij}\ (a^*) = \frac{\partial f_\rho^i(a^*)}{\partial a_j} = w_{ij}\,\sigma'\,(a_j^*), \qquad i,\ j = 1, \ldots, n. \tag{4}$$

A fixed point $a^* \in \mathcal{A}$ is an attractor of a given n-module if all eigenvalues λ_i of $Df_\rho\ (a^*)$ have modulus less than one; i.e. $|\,\lambda_i\,| < 1, i = 1, \ldots, n$. One may then use theorems like the Banach contraction principle [36] or Schur-D-stability [37] of the linearization Df_ρ to determine the uninteresting parameter domains.

In addition, considering an appropriate equivalence class of neuromodules instead of a particular network configuration will be desirable. A standard definition is the following: two dynamical systems $(\mathcal{A}, f)$, $(\mathcal{B}, g)$ are called *topologically conjugate*, if there exists a homeomorphism $h : \mathcal{A} \to \mathcal{B}$, such that $g \circ h = h \circ f$. To classify the n-modules as parametrized families of dynamical systems we use the following definition.

Definition 1. *Two n-modules $(\mathcal{A}, f_\rho)$, $(\mathcal{B}, g_{\rho'})$ with $\rho \in \mathcal{Q}$, $\rho' \in \mathcal{Q}'$, are called dynamically equivalent, if there exists a map $T : \mathcal{Q} \to \mathcal{Q}'$, such that with $\rho' = T(\rho)$ the dynamical systems f_ρ and $g_{\rho'}$ are topological conjugate; i.e. there exists a homeomorphism $\phi : \mathcal{A} \to \mathcal{B}$ such that the following diagram commutes:*

$$\begin{array}{ccccc} & & & f_\rho & \\ & \mathcal{Q} \times \mathcal{A} & \longrightarrow & \mathcal{A} & \\ T \times \phi & \downarrow & & \downarrow & \phi \\ & \mathcal{Q}' \times \mathcal{B} & \longrightarrow & \mathcal{B} & \\ & & & g_{\rho'} & \end{array}$$

For example one may define the *flip operators* $I_k : \mathcal{A} \to \mathcal{A}$, $k = 1, \ldots, n$ acting on the kth component of a state vector $a \in \mathcal{A}$ as a sign reflection

$$(I_k\ a)_j = \begin{cases} a_j & \text{if } k \neq j, \\ -a_j & \text{if } k = j. \end{cases} \tag{5}$$

Using the symmetry of the sigmoid (2), given by $\sigma(-x) = (1 - \sigma(x))$, it is easy to prove the following by direct calculation. For every neuromodule with n neurons there exists in principle a set of 2^n parameter vectors, all leading to qualitatively the same dynamical behaviour. We have the following lemma.

Lemma 1. *Given an n-neuromodule $(\mathcal{A}, f_\rho)$, $\rho \in \mathcal{Q} \subset \boldsymbol{R}^q$. If the activity dynamics (1) of the module is changed by a sign reflection operator $I_k : \mathcal{A} \to \mathcal{A}$, then there exists an induced transformation $T_k : \mathcal{Q} \to \mathcal{Q}$ on the parameter space $\mathcal{Q}$, such that with $\rho' := T_k(\rho)$ the dynamical system $(\mathcal{A}, f_{\rho'})$ is topological conjugate to $(\mathcal{A}, f_\rho)$; i.e. $I_k \circ f_\rho = f_{\rho'} \circ I_k$.*

The action of the induced transformations T_k on $\mathcal{Q}$ is given by

$$(T_k\,\theta)_i = \begin{cases} \theta_i + w_{ik} & \text{if } k \neq i, \\ -\theta_i - w_{ii} & \text{if } k = i, \end{cases} \tag{6}$$

$$(T_k\,w)_{ij} = \begin{cases} -w_{ij} & \text{if } (k = i \text{ or } j) \text{ and } i \neq j, \\ w_{ij} & \text{else.} \end{cases} \tag{7}$$

Equations (6) and (7) show that transformations $T_k : \mathcal{Q} \to \mathcal{Q}$ associated with flip operators I_k on $\mathcal{A}$ simultaneously change the sign of all input and output connections of neuron k, except its self-connection, which is invariant under T_k.

Furthermore, it should be noted that changing the sigmoidal transfer function, for instance from the standard sigmoid σ, as given by equation (2), to tanh, will also lead to dynamically equivalent n-modules. This again can be proven by direct calculation using the relation $\tanh(x) = 2\sigma(2x) - 1$.

The guiding idea for finding parameter domains associated with complex neural dynamics, in the sense described above, is the following: given an n-module $(\mathcal{A}, f_\rho)$ with dynamics bounded to a domain $\mathcal{U} \subset \mathcal{A}$. Let Df_ρ denote the Jacobian of this system. Then $(\mathcal{A}, f_\rho)$ can display complex dynamics, if there exists a parameter vector $\rho \in \mathcal{Q}$ and a state $a^* \in \mathcal{U}$ such that at least for one row i of Df_ρ the row sum is zero, i.e.

$$\sum_{j=1}^{n} (Df_\rho)_{ij}\ (a^*) = \sum_{j=1}^{n} w_{ij}\, \sigma(a_j^*) = 0. \tag{8}$$

Of course, the existence of isolated neurons (all $w_{ij} = 0$) is excluded.

The essential statement of this criterion is of course that at least one neuron in the network has to receive an excitatory as well as an inhibitory input. In the form of equation (8) it is suggested by the many observations made by simulating the dynamics of recurrent neural networks. Mathematically it states the following: if $X = (1, \ldots, 1)$ denotes the constant vector field on $\mathcal{A}$ pointing in the direction of the main diagonal in $\boldsymbol{R}^n$, then the Lie-derivative (i.e. the directional derivative) $L(X)\ f_\rho^i$ of some component i of the map f_ρ in the direction of X must vanish for some $a^* \in \mathcal{U}$.

From lemma 1 we know that the dynamics does not change qualitatively if we change the sign of all input and output connections (without a possible self-connection) of a neuron simultaneously. We therefore define functions Inv_i, $i = 1, \ldots, n$, on $\mathcal{A}$, which are invariant under the action of flip operators, by

$$\mathrm{Inv}_i\ (a) := \sigma'(a_i) \sum_{j=1}^{n} w_{ij} w_{ji} \sigma'(a_j), \qquad a \in \mathcal{U}, i = 1, \ldots, n. \tag{9}$$

This so-called *first loop function* of neuron i is the contraction of the ith column vector with the ith row vector of the linearization Df_ρ.

The criterion (8) turned out to be a good guide to parameter domains were complex dynamics can occur; at least higher-periodic up to quasi-periodic attractors have been found in corresponding networks. But there are examples where this equation still holds, but there is no chaos, or at least no period-doubling route to chaos observed. For the existence of chaos it seems, that in addition to equation (8) the following has to be satisfied: there exists a parameter vector $\rho \in \mathcal{Q}$ and a state $a \in \mathcal{U}$, different from that of equation (8), such that $\mathrm{Inv}_i\ (a) = 0$ holds for the same i as in equation (8). For fixed i, and $w_{ij} w_{ji} = 0$ not for all j, with equation (9) this corresponds to

$$\sum_{j=1}^{n} w_{ij} w_{ji} \sigma'(a_j) = 0. \tag{10}$$

This condition postulates the existence of at least one neuron i in the network for which at least two loops interact in a competitive way. These loops can be a self-connection w_{ij} and/or two-neuron loops. They then must feed neuron i with opposite signs.

Both conditions (8) and (10) turned out to be satisfied simultaneously whenever chaotic dynamics appeared in the considered cases of two- and three-dimensional neuro-dynamics. Because they represent global properties of neuromodules, they presumably cannot be expressed alone in terms of the linearization Df_ρ, which describes only local properties. On the other hand, it is obvious from the simulations that the type of loops (i.e. consisting of an even or

odd number of inhibitory connections) together with the length of loops play an essential role for what type of dynamical features are accessible. Thus, equations (8) and (10) probably refer only to a special case of a more general condition for higher dimensions. Respecting the first condition (8), the following example networks will have excitatory and inhibitory neurons.

3. The chaotic two-neuron module

The simplest neuromodule to discuss is a network of two neurons. In general, its dynamics is given by a six-parameter family of maps $f_\rho : \boldsymbol{R}^2 \to \boldsymbol{R}^2$, $\rho = (\theta_1, w_{12}, w_{11}, \theta_2, w_{21}, w_{22}) \in \boldsymbol{R}^6$, but for simplicity one may set $w_{22} = 0$ in the following. Thus we will discuss the dynamics defined by

$$\begin{aligned} a_1(t+1) &:= \theta_1 + w_{11}\,\sigma(a_1(t)) + w_{12}\,\sigma(a_2(t)), \\ a_2(t+1) &:= \theta_2 + w_{21}\,\sigma(a_1(t)). \end{aligned} \tag{11}$$

This configuration is known to allow also chaotic dynamics for some parameter values $\rho \in \boldsymbol{R}^5$ (see, for example, [24]), and we will therefore call it a *chaotic 2-module*. To test our criteria for complex dynamics we first observe that condition (8) can be satisfied for the first row of the linearization of this neuromodule, i.e.

$$w_{11}\sigma'(a_1) + w_{12}\sigma'(a_2) = 0$$

for some $a \in \mathcal{A}$, if and only if $w_{11}w_{12} < 0$, because $\sigma' > 0$ is a strictly positive function. Of course, the necessary range of activities a_1 and a_2 can be chosen by fixing corresponding bias terms θ_1 and θ_2 conveniently. We will use a self-inhibitory neuron here; i.e. $w_{11} < 0$. The condition (10) now reads

$$w_{11}^2\sigma'(a_1) + w_{12}w_{21}\sigma'(a_2) = 0$$

for some $a \in \mathcal{A}$. This can be satisfied only if $w_{12}w_{21} < 0$, and for respecting Dale's rule we choose $w_{21} < 0$. Thus, we consider the dynamics of a two-neuron network consisting of an excitatory and an inhibitory unit. Without self-connections ($w_{11} = w_{22} = 0$) the resulting recurrent feedback loop has, besides parameter domains for which there exist global fixed point attractors, parameter domains where two fixed point attractors co-exist with a period-2 attractor ($w_{12}w_{21} > 0$) and another domain where there is a global period-4 attractor ($w_{12}w_{21} < 0$) [38]. A rough sketch of the complex dynamical properties of the 2-module can be found in the so-called iso-periodic plot of figure 1, where colour coded we find the periodic attractors existing for corresponding points in the two-dimensional (w_{11}, w_{12})-parameter subspace.

At this point we may remark that, according to lemma 1, the dynamics of this module is topologically conjugate for the following four parameter vectors:

$$\rho_1 := (\theta_1,\ w_{11},\ w_{12},\ \theta_2,\ w_{21}), \tag{12}$$

$$\rho_2 := (-(\theta_1 + w_{11}),\ w_{11},\ -w_{12},\ (\theta_2 + w_{21}),\ -w_{21}), \tag{13}$$

$$\rho_3 := ((\theta_1 + w_{12}),\ w_{11},\ -w_{12},\ -\theta_2,\ -w_{21}), \tag{14}$$

$$\rho_4 := (-(\theta_1 + w_{11} + w_{12}),\ w_{11},\ w_{12},\ -(\theta_2 + w_{21}),\ w_{21}), \tag{15}$$

where $\rho_2 = T_1(\rho_1)$, $\rho_3 = T_2(\rho_1)$, and $\rho_4 = T_1 \circ T_2(\rho_1) = T_2 \circ T_1(\rho_1)$.

Interesting dynamical parameter domains will be those, for which all stationary states are unstable. So we will look for the set of all fixed points a^* such that the Jacobian $Df_\rho(a^*)$ of the dynamics f at a^* has at least one eigenvalue with modulus larger than one. The fixed point equations reads

$$a_i^* = \theta_i + \sum_{j=1}^{2} w_{ij}\,\sigma(a_j^*(t)), \qquad i = 1, 2, \tag{16}$$

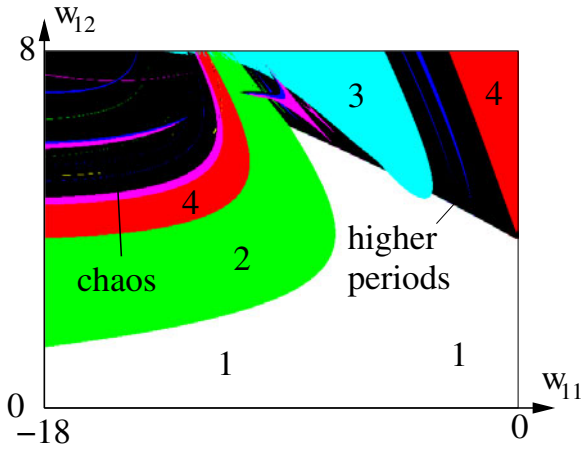

Figure 1. Chaotic 2-module: iso-periodic plot in the (w_{11}, w_{12})-subspace for fixed parameters $w_{21} = -6, \theta_1 = -3, \theta_2 = 4$. Numbers r refer to the existence of period-r attractors.

and the Jacobian $Df_\rho(a^*)$ of the dynamics (11) with $w_{22} = 0$ is given by

$$Df_\rho(a^*) = \begin{pmatrix} w_{11}\sigma'(a_1^*) & w_{12}\sigma'(a_2^*) \\ w_{21}\sigma'(a_1^*) & 0 \end{pmatrix}. \tag{17}$$

We will discuss stability criteria for the stationary states [39] in terms of the trace $\mathcal{T}$ and the determinant $\mathcal{D}$ of $Df_\rho(a^*)$, which are here given by

$$\mathcal{T} = w_{11}\sigma'(a_1^*), \qquad \mathcal{D} = -w_{12}w_{21}\sigma'(a_1^*)\sigma'(a_2^*).$$

The eigenvalues of $Df_\rho(a^*)$ are then given by

$$\lambda_{1,2} = \tfrac{1}{2}\left(\mathcal{T} \pm \sqrt{\mathcal{T}^2 - 4\mathcal{D}}\right).$$

The domain of stability for a fixed point a^* in the $(\mathcal{T}, \mathcal{D})$-plane is given by a triangle bounded by the three straight lines $T - D = 1$, $T + D = -1$, and $D = 1$ [39]. For the case considered here, i.e. $w_{11} \leqslant 0$, $w_{21} < 0$ and $w_{12} > 0$, we have

$$-|w_{11}| < \mathcal{T} < 0, \qquad 0 < \mathcal{D} < |w_{12}\, w_{21}|\, \sigma'(a_1^*)\, \sigma'(a_2^*). \tag{18}$$

Thus, at least two types of bifurcations have to be expected: along the line $\mathcal{T} + \mathcal{D} = -1$ there will be a period-doubling or *flip* bifurcation from a fixed point attractor to a period-2 attractor; along the line $\mathcal{D} = 1$, $|\mathcal{T}| < 2$ there will be a Neimark–Sacker bifurcation from a fixed point attractor to a periodic or quasiperiodic attractor [39].

In general, the eigenvalues $\lambda_{1,2}\,(a^*)$ are functions not only of the weights w_{ij} but also of the bias terms θ_i, i.e. of all five parameters. This makes a deeper analytical treatment of the bifurcation behaviour very difficult [30]. But to get an idea how the structure observed in figure 1 is generated we may look instead for the stability of the origin $(0, 0) \in \boldsymbol{R}^2$ which is a fixed point for parameters satisfying

$$\theta_1 = -\tfrac{1}{2}\,(w_{11} + w_{12}), \qquad \theta_2 = -\tfrac{1}{2}\,w_{21}. \tag{19}$$

For this stationary state we get from equations (18) and $\sigma(0) = 0.5$

$$\mathcal{T} = \tfrac{1}{4}\,w_{11}, \qquad \mathcal{D} = -\tfrac{1}{16}\,w_{12}\,w_{21}.$$

So, a flip bifurcation will appear if the weights satisfy the following equations:

$$4w_{11} - w_{12}\,w_{21} = -16,$$

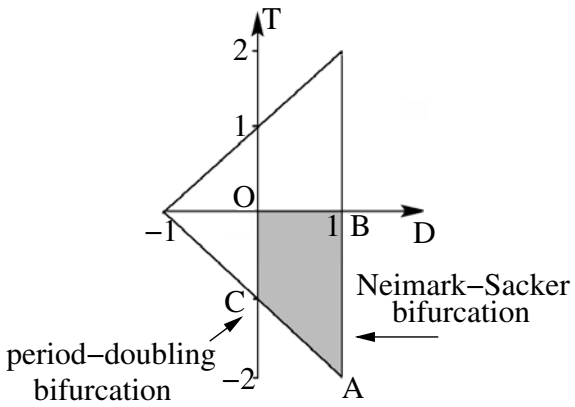

Figure 2. The stability domain for a fixed point in terms of trace $\mathcal{T}$ and determinant $\mathcal{D}$ of the linearization Df_ρ; the shaded domain corresponds to recurrent coupling of a self-inhibitory with an excitatory neuron.

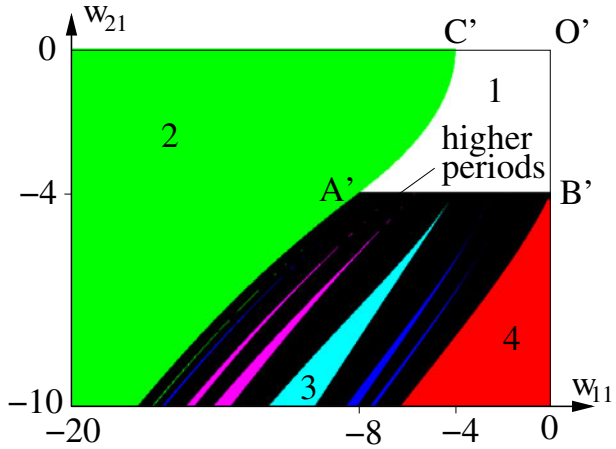

Figure 3. Chaotic 2-module: iso-periodic plot in the (w_{11}, w_{12})-subspace for $w_{12} = -w_{21}$, $\theta_1 = -0.5\,(w_{11} + w_{12})$, $\theta_2 = -0.5\,w_{21}$. For these parameter values the origin in activity space is always a stationary state. Numbers r refer to the existence of period-r attractors.

and the Neimark–Sacker bifurcation will occur for

$$|\,w_{11}\,| < 8, \qquad |\,w_{12}\;w_{21}\,| = 16.$$

To compare these results with the iso-periodic plot in the (w_{11}, w_{12})-plane shown in figure 3, where now in addition to equation (19) we set $w_{21} = -w_{12}$, we obtain for the flip bifurcation set

$$w_{12} = 2\sqrt{-4 - w_{11}}, \qquad -8 \leqslant w_{11} \leqslant -4, \tag{20}$$

and, correspondingly, for the Neimark–Sacker bifurcation set we get the straight line

$$w_{12} = 4, \qquad -8 < w_{11} < 0. \tag{21}$$

The corners of stability domain in the $(\mathcal{D}, \mathcal{T})$-space $O = (0, 0)$, $A := (1, -2)$, $B := (1, 0)$, $C := (0, -1)$ in figure 2 correspond to the points O', A', B', C' in (w_{11}, w_{12})-parameter subspace of figure 3: points B, B' correspond to a bifurcation from a fixed point

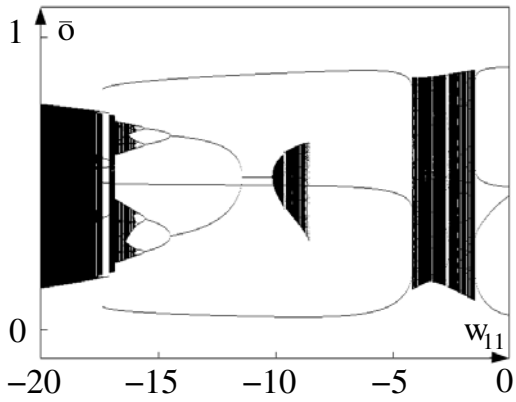

Figure 4. Chaotic 2-module: bifurcation sequence for varying self-connection w_{11} of the 2-module with $\theta_1 = -3.8$, $\theta_2 = 3$, $w_{12} = 5.9$, $w_{21} = -6.6$. Plotted is the averaged output $\overline{o}$ of the module.

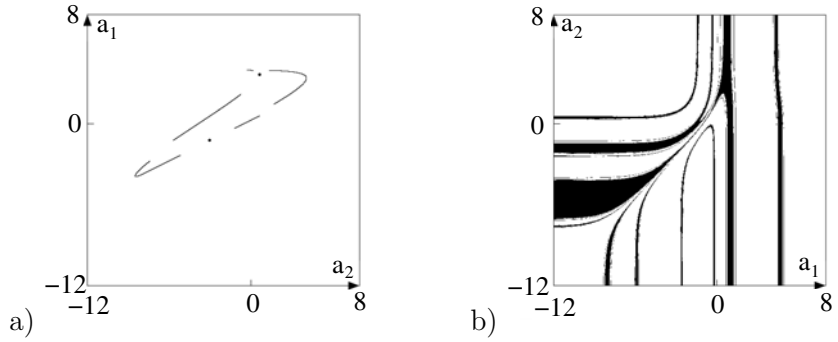

Figure 5. Chaotic 2-module: (*a*) a period-2 attractor co-existing with a cyclic chaotic attractor in (a_1, a_2)-activity space. (*b*) Basins of period-2 attractor (black) and chaotic attractor (white) with fractal basin boundaries for parameter values $\theta_1 = -0.45$, $\theta_2 = 3.9$, $w_{11} = -16$, $w_{12} = 8$, $w_{21} = -8$.

attractor to a global period-4 attractor observed for an odd two-ring network [38], points C, C' correspond to a single self-inhibitory neuron bifurcating from a stable fixed point to a stable period-2 orbit [33]. Of course, the lines AB and AC of the stability domain $OABC$ are mapped to the bifurcation sets $\overline{A'B'}$ and $\overline{A'C'}$, given by equations (20) and (21), correspondingly. In general, the components of a fixed point a^* depend on all five parameters of the system (11), and generically they will satisfy $a_i^* \neq 0$, $i, \ldots, n$, i.e. we have $\sigma'(a_i^*) < \sigma'(0) = 0.25$. Thus, the stability domain $O'A'B'C'$ will be smoothly deformed, and, correspondingly, the bifurcation sets $\overline{A'B'}$ and $\overline{A'C'}$ will be smoothly deformed with smoothly varying fixed points a^*. And for $w_{12} = -w_{21}$ complex dynamics will be found only outside of these stability domains.

Especially, figure 1 shows the existence of larger parameter domains where period-3 attractors are dominant. In these period-3 domains there often co-exists a whole cascade of period-doubling bifurcations to chaos with a period-3 attractor (compare figure 4). And there are also Neimark–Sacker bifurcations from fixed points to quasiperiodic attractors co-existing with stable period-3 orbits in these domains. These bifurcation diagrams are obtained by multiple passes using different fixed initial conditions. The averaged outputs $\overline{o} := \frac{1}{n}\sum_{i=1}^{n} o_i$ of the actual network are plotted. For instance, figure 4 reveals a period-3 attractor co-existing with a period doubling route to chaos in the domain $-17.4 < w_{11} < -11.4$,

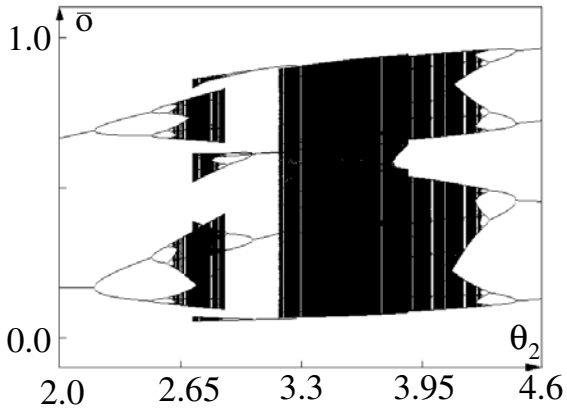

Figure 6. Chaotic 2-module: bifurcation sequence for θ_2 of the chaotic 2-module with $\theta_1 = -1.74$, $w_{11} = -16$, $w_{12} = 6$, $w_{21} = -6$, indicating co-existing chaotic attractors around $\theta_2 = 2.75$. Plotted is the averaged output $\bar{o}$ of the module.

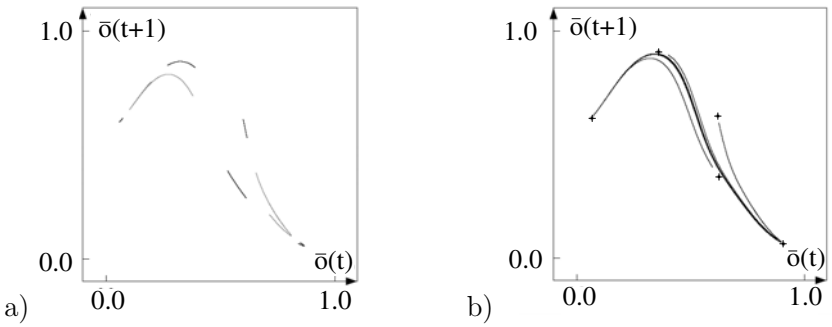

Figure 7. Chaotic 2-module: for parameters $\theta_1 = -1.75$, $w_{11} = -16$, $w_{12} = 6$, $w_{21} = -6$ one observes (*a*) a 2-cyclic chaotic attractor (grey) co-existing with a 5-cyclic one (black) for $\theta_2 = 2.78$, and (*b*) a chaotic attractor co-existing with a period-5 attractor (stars) for $\theta_2 = 3.25$, displayed in terms of the first return map of the averaged output $\bar{o}$.

then a fixed point attractor for $-11.4 < w_{11} < -10.1$ and a domain of quasi-periodic and higher periodic attractors between $-10.1 < w_{11} < -8.5$. A domain of global quasi-periodic and higher periodic attractors also exists between $-4.2 < w_{11} < -1.5$ followed by global period-4 attractors. Noticeable is also a *generalized hysteresis effect* over the whole interval $-17.4 < w_{11} < -1.5$: starting with a chaotic attractor, crossing this hysteresis interval with w_{11} increasing, a period doubling route is followed backward to a fixed point attractor and to quasi-periodic and periodic attractors with the system suddenly jumping into the period-3 attractor. Crossing the interval now again with w_{11} decreasing only the period-3 will appear until the system jumps back to a chaotic attractor around $w_{11} = -17.4$.

Although the basin structure of co-existing chaotic and period-3 attractors seems to be quite regular in general, there also exist chaotic attractors together with period-2 orbits, having fractal basin boundaries. An example is given in figures 5(*a*) and (*b*) for the parameter values $\theta_1 = -0.45, \theta_2 = 3.9, w_{11} = -16, w_{12} = 8, w_{21} = -8$. The existence of even more complex dynamical behaviour can be detected in the bifurcation sequence for the parameter θ_2 shown in figure 6; the other parameters are fixed as follows: $\theta_1 = -1.74$, $w_{11} = -16$, $w_{12} = 6$,

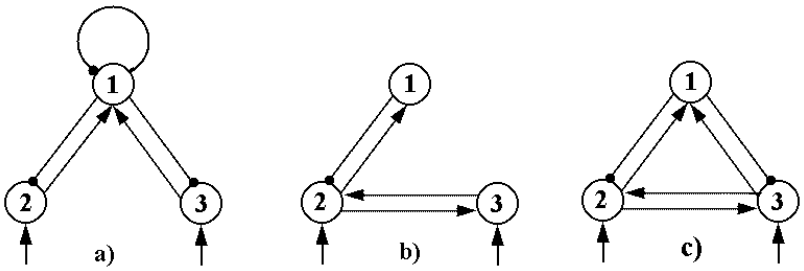

Figure 8. Three examples of three-neuron modules, all with one inhibitory neuron. Arrows denote excitatory, dots inhibitory connections.

$w_{21} = -6$. To analyse this situation recall, that a chaotic attractor is called *p-cyclic*, if it has p connected components which are permuted cyclically by the map f_ρ. Every component of a p-cyclic attractor is an attractor of the pth iterate f_ρ^p [40].

Now, over the interval $2.72 < \theta_2 < 2.9$ there co-exist two different chaotic attractors. One is 2-cyclic, the other is 5-cyclic. Both are shown in figure 7(*a*). Thus, over this interval we observe a generalized hysteresis effect, switching between two different cyclic chaotic behaviours. A second hysteresis interval $3.18 > \theta_2 > 3.28$ can be seen, where a chaotic attractor co-exists with a period-5 attractor. This configuration is depicted in 7(*b*).

4. Three-neuron modules

In this section we will discuss different types of three-neuron modules. According to our guide line, for producing interesting dynamical properties these modules should have at least one neuron getting excitatory as well as inhibitory inputs. This can be realized, for example, by the three configurations shown in figure 8. The first one has a self-inhibiting neuron in the middle of a bi-directional 3-chain. The second one uses an inhibitory neuron at one end of such a chain. The third configuration is a bi-directional 3-ring with one inhibitory neuron. All these configurations can display chaotic dynamics.

According to lemma 1 there are many more three-neuron configurations, which are dynamically equivalent (definition 1) to these three examples. But there are even more equivalence classes. For instance, one which is represented by a three-neuron uni-directional ring network with one neuron having a self-connection.

4.1. A 3-chain with self-inhibiting centre neuron

This module is described as a discrete-time dynamical system with eight parameters given by

$$\begin{aligned} a_1(t+1) &:= \theta_1 + w_{11}\,\sigma(a_1(t)) + w_{12}\,\sigma(a_2(t)) + w_{13}\,\sigma(a_3(t)), \\ a_2(t+1) &:= \theta_2 + w_{21}\,\sigma(a_1(t)), \\ a_3(t+1) &:= \theta_3 + w_{31}\,\sigma(a_1(t)). \end{aligned} \tag{22}$$

To go to dynamically interesting parameter domains for this configuration the first condition (8) of the complex dynamics criterion

$$w_{11}\sigma'(a_1) + w_{12}\sigma'(a_2) + w_{13}\sigma'(a_3) = 0$$

can be satisfied if we assume for the first row of the linearization $w_{11} < 0$ and $w_{12}\,, w_{13} > 0$. Then the bias terms can be arranged in such a way, so that this condition holds. The chaos condition (10) now reads

$$\mathrm{Inv}_1 = w_{11}^2\sigma'(a_1) + w_{12}w_{21}\sigma'(a_2) + w_{13}w_{31}\sigma'(a_3) = 0,$$

for some $a \in \mathcal{A}$. This can be satisfied only if $w_{12}w_{21} < 0$ and/or $w_{13}w_{23} < 0$, and for respecting Dale's rule we choose $w_{21},\ w_{31} < 0$. Thus, we consider the dynamics of a self-inhibiting neuron coupled bi-directionally to two excitatory neurons as shown in figure 8(a).

It can be easily shown that the three-dimensional dynamics (22) is essentially a two-dimensional one, living on a two-dimensional sub-manifold in three-dimensional activity space $\mathcal{A}$. This is the case, because neurons 2 and 3 are synchronized in the general sense [41]; i.e. their activities are related by the equation

$$a_3(t) = \theta_3 + \frac{w_{31}}{w_{21}}(a_2(t) - \theta_2). \tag{23}$$

Although the 3-module (22) is effectively a two-dimensional systems, it can of course not be reduced to a two-neuron network. This can be done only in the special case, for which the excitatory neurons 2 and 3 are synchronized, i.e. $a_2(t) = a_3(t)$ for all $t > t_0$. This is realized if and only if the following *synchronization condition* is satisfied:

$$\theta_2 = \theta_3, \qquad w_{21} = w_{31}. \tag{24}$$

Then the dynamics (22) of the module reduces to the dynamics (11) of a two-neuron network A having a connection $w_{12}^A = (w_{12} + w_{13})$.

Suppose the eight parameters in the dynamics (22) satisfy

$$-2\theta_1 = (w_{11} + w_{12} + w_{13}), \qquad -2\theta_2 = w_{21}, \qquad -2\theta_3 = w_{31}. \tag{25}$$

Consequently, the origin $a^* = (0, 0, 0)$ is a stationary state, and the eigenvalues of the linearization $Df_\rho(a^*)$ at a^* are given by

$$\lambda_1(0) = 0, \qquad \lambda_{2,3}(0) = \tfrac{1}{8}\left(w_{11} \pm \sqrt{w_{11}^2 - 4\,(w_{12}w_{21} + w_{13}w_{31})}\right).$$

The stationary state a^* will become non-hyperbolic if one of these eigenvalues has modulus 1. Because $w_{12}w_{21} < 0$ and $w_{13}w_{31} < 0$ (both loops are odd) there will be only real eigenvalues, and the bifurcation sets in parameter space are defined by

$$16 + (w_{12}w_{21} + w_{13}w_{31}) \pm 4\,w_{11} = 0.$$

For the special case where, in addition to equation (25), parameters also satisfy $w_{21} = w_{31}$ and $w_{12} = w_{13} = 4$, an iso-periodic plot in the (w_{11}, w_{21})-parameter subspace is depicted in figure 9. In this figure the line $\overline{AC}$ corresponds to period-doubling bifurcations, and the line $\overline{AB}$ to Neimark–Sacker bifurcations. Points have coordinates $A = (-8, -2)$, $B = (0. - 2)$, $C = (-4, 0)$. Because the dynamics of the module is essentially a two-dimensional one—as was stated above—this figure is clearly equivalent to that of the 2-module in figure 3.

According to lemma 1, there are now in general eight different parameter vectors $\rho \in \boldsymbol{R}^8$ generated by the basic transformation T_k, $k = 1, 2, 3$, all giving topologically conjugate dynamics. Knowing that for $\theta_2 = \theta_3$, $w_{21} = w_{31}$ the module dynamics reduces to the known two-dimensional one, we may ask what happens if $\theta_2 \neq \theta_3$. So, for a first simulation, shown again in terms of an iso-periodic plot for the (θ_2, θ_3)-parameter space in figure 10, we choose $w_{12} = w_{13} = 4$, $w_{21} = w_{31} = -6$, $w_{11} = -16$ and $\theta_1 = -3.4$.

We observe that the three-dimensional dynamics around the main diagonal, which corresponds to the synchronization condition (24) for neurons 2 and 3, has qualitatively the same properties as the chaotic two-neuron module: besides fixed point attractors, we have large domains for period-2 and period-3 attractors, period doubling routes to chaos, also co-existing with period-3 attractors in the middle of the figure, and domains for higher periodic and quasi-periodic attractors crossing the θ_1- and θ_2-axes.

The synchronization condition (24) is violated for the situation depicted in figure 11 where an iso-period plot in the (θ_2, w_{21})-parameter space is shown for $\theta_1 = -2$, $\theta_3 = 3.4$,

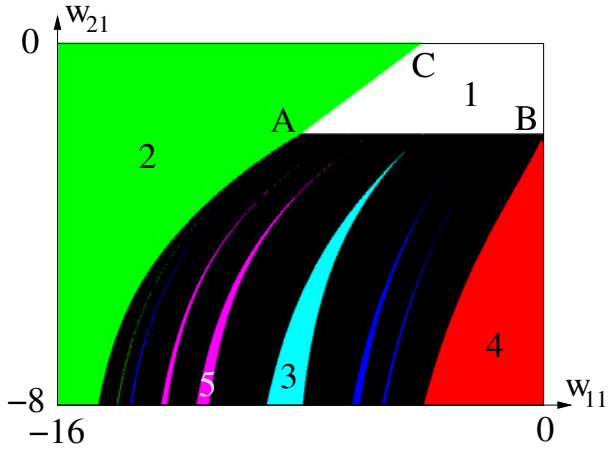

Figure 9. 3-chain 4.1: iso-periodic plot in the (w_{11}, w_{21})-parameter subspace for which the origin $a^* = 0$ is always a fixed point (see the text for parameters). Numbers r refer to the existence of period-r attractors.

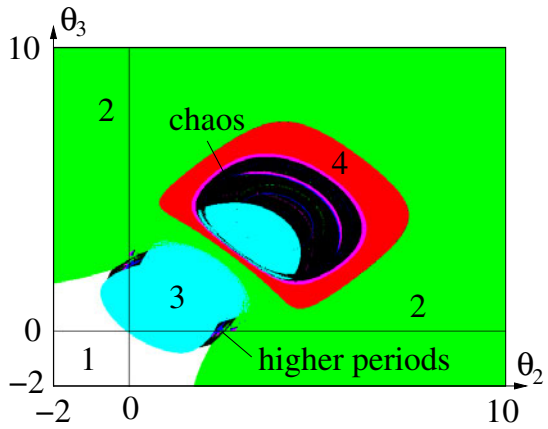

Figure 10. 3-chain 4.1: iso-periodic plot for (θ_2, θ_3)-parameter subspace for $w_{12} = w_{13} = 4$, $w_{21} = w_{31} = -6$, $w_{11} = -16$, $\theta_1 = -3.4$ fixed. Numbers r refer to the existence of period-r attractors.

$w_{11} = -16$, $w_{21} = w_{31} = -6$, $w_{13} = 4$. Again we find the typical dynamical properties like period-doubling routes to chaos, higher- and quasi-periodic attractors and large period-3 domains as described before.

4.2. 3-chain with inhibitory an neuron at one end

The second three-neuron module corresponds to a bi-directional 3-chain with an inhibitory neuron at one end (figure 8(*b*)). Its discrete dynamics is given by a seven-parameter family of maps $f_\rho : \boldsymbol{R}^3 \to \boldsymbol{R}^3$ defined by

$$\begin{aligned} a_1(t+1) &:= \theta_1 + w_{12}\,\sigma(a_2(t)), \\ a_2(t+1) &:= \theta_2 + w_{21}\,\sigma(a_1(t)) + w_{23}\,\sigma(a_3(t)), \\ a_3(t+1) &:= \theta_3 + w_{32}\,\sigma(a_2(t)). \end{aligned} \tag{26}$$

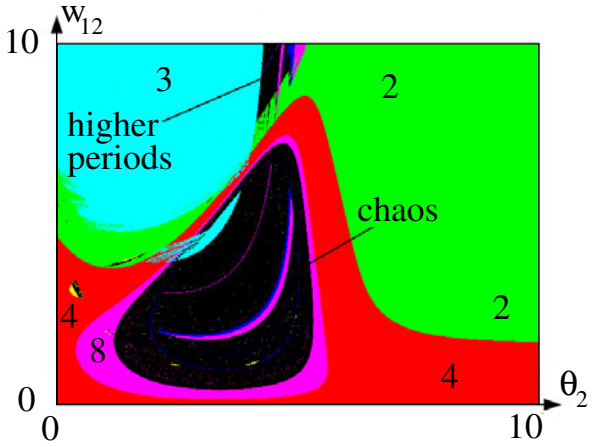

Figure 11. 3-chain 4.1: iso-periodic plot for (θ_2, w_{21})-parameters with $\theta_1 = -2$, $\theta_3 = 3.4$, $w_{11} = -16$, $w_{21} = w_{31} = -6$, $w_{13} = 4$ fixed. Numbers r refer to the existence of period-r attractors.

A complex dynamics condition (8) for this configuration is given for neuron 2 by

$$w_{21}\,\sigma'(a_1) + w_{23}\,\sigma'(a_3) = 0,$$

and it can be satisfied with $w_{21}w_{23} < 0$ by adjusting the corresponding bias terms. In the following we choose neuron 1 to be inhibitory, i.e. $w_{21} < 0$. The chaos condition (10) for the second component reads

$$\mathrm{Inv}_2 = w_{12}w_{21}\,\sigma'(a_1) + w_{23}w_{32}\,\sigma'(a_3) = 0,$$

for some $a \in \mathcal{A}$ in this case. Having chosen $w_{21} < 0$ we will set all other connections to be excitatory: $w_{12},\ w_{23},\ w_{32} > 0$. Thus, for satisfying Dale's rule we have chosen a bi-directional 3-chain with an inhibitory neuron at one end (figure 8(*b*)).

Due to lemma 1 this dynamics f_ρ (26) is now topologically conjugate to that of eight other parameter vectors $\rho' \in \boldsymbol{R}^7$ generated again by the basic transformations T_k, $k = 1,\ 2,\ 3$ of equations (6), (7). Furthermore, the dynamics of this module is again essentially a two-dimensional one, because now the neurons 1 and 3 are synchronized in a general sense [41]; i.e. their activities are related by the equation

$$a_3(t) = \theta_3 + \frac{w_{32}}{w_{12}}(a_1(t) - \theta_1). \tag{27}$$

This can be seen, for instance, in figure 15, where the projection onto the (o_1, o_3)-subspace of a chaotic attractor appears to be one dimensional. Although the dynamic of this module is again two dimensional, its dynamics seems to be more complex than that of the last module (22) as will be discussed next.

The point $a^* = (0, 0, 0)$ is always a fixed point of the dynamics (26), if the parameters satisfy $-2\theta_1 = w_{12}$, $-2\theta_2 = w_{21} + w_{23}$, and $-2\theta_3 = w_{32}$. It becomes non-hyperbolic if one of the eigenvalues

$$\lambda_{2,3}(0) = \pm\tfrac{1}{4}\sqrt{w_{12}w_{21} + w_{23}w_{32}}$$

has modulus 1. The first eigenvalue $\lambda_1(0)$ is always zero.

To study dynamically interesting parameter domains we now choose competing even and odd loops, i.e. $w_{12}w_{21} < 0$ and $w_{23}w_{32} > 0$. The appearance of periodic and chaotic

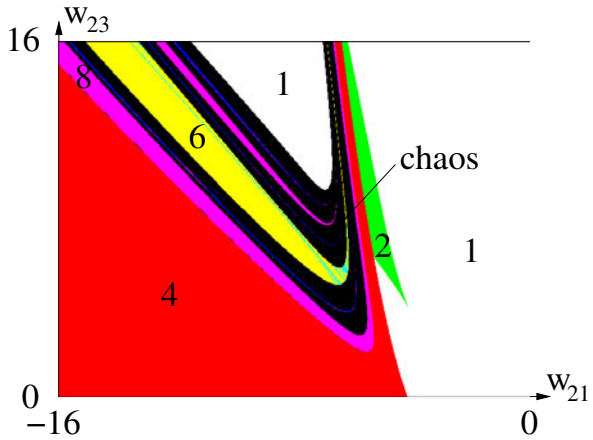

Figure 12. 3-chain 4.2: iso-periodic plot in the (w_{21}, w_{23})-parameter subspace with fixed parameters $w_{12} = w_{32} = 8$, $\theta_1 = -3$, $\theta_2 = 3.95$, $\theta_3 = -7$. Numbers r refer to the existence of period-r attractors.

parameter domains is revealed, for instance, in figure 12 for the (w_{23}, w_{21})-parameter subspace. Following Dale's rule the other five parameters are fixed conveniently as follows: $\theta_1 = -3$, $\theta_2 = 3.95$, $\theta_3 = -7$, $w_{12} = w_{32} = 8$.

We will not describe the dynamics as detailed as for the 2-module: we observe mainly the same features: periodic and quasi-periodic attractors, period doubling routes to chaos, etc. What is new for this three-neuron module is its even greater complexity: here we not only observe one period-doubling sequence, but co-existing period-doubling routes to chaos leading to co-existing chaotic attractors. For example, figure 12 indicates period-doubling to chaos (black domain) starting from period-4 orbit attractors indicated by the red domain. In fact, simulations show, that the period-4 attractor bifurcates into two period-8 attractors, inducing two separated routes to chaos.

The same holds for the period-6 domain given in figure 12 included in the chaotic region: it stands for co-existing period-3 and period-6 attractors bifurcating along different routes to chaos. After staying separate for a while, these co-existing chaotic attractors experience an *attractor merging crisis* at specific parameter values; i.e. they end up in one attractor.

For $w_{21} > 4$ there is a cusp-shaped region of period-2 attractors that, for decreasing w_{23}, undergoes period-doubling to chaos. All these different routes to chaos co-exist in parameter domains around $w_{23} = 7$ and $w_{21} > 8$. This complicated dynamical properties are clearly visible in the bifurcation diagram of figure 13 for θ_2. Here the weights are fixed at $-w_{21} = w_{23} = w_{12} = w_{32} = 8$, and bias terms at $\theta_1 = -3, \theta_3 = -7$. Starting with $\theta_2 = 8$ we have a global fixed point attractor. With θ_2 decreasing, at $\theta_2 = 6.72$ a period-2 (marked by β) and a fixed point attractor (marked by α) appear in addition. At $\theta_2 = 6.23$ co-existing period-doubling routes to chaos start with the period-2 attractor bifurcating into a period-4 orbit and the fixed point attractor bifurcating with a strong resonance of order 4 also into period-4 attractors. The upper sequence (starting from the period-2 orbit) vanishes together with the fixed point attractor at $\theta_2 = 5.63$ and only the lower sequence remains, ending up in a period-4 orbit around $\theta_2 = 2.35$. These period-4 attractors appear through a strong resonance bifurcation of order 4 from a global fixed point at $\theta_2 = -0.58$. We notice, that for this configuration there exists a general hysteresis phenomenon over the interval $5.63 < \theta_2 < 6.72$, where a whole period-doubling route to chaos and a fixed point attractor is involved: crossing this

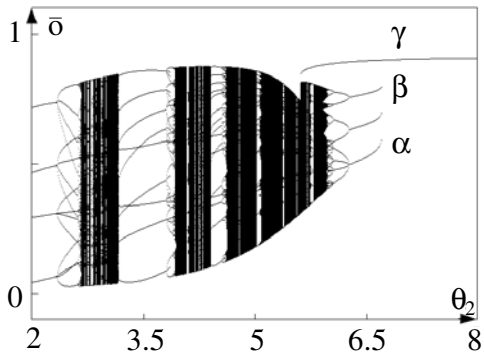

Figure 13. 3-chain 4.2: bifurcation sequence for θ_2 and fixed parameters $-w_{21} = w_{23} = w_{12} = w_{32} = 8$, $\theta_1 = -3$, $\theta_3 = -7$. Plotted is the mean output $\overline{o}$ of the module. The diagram indicates the co-existence of different attractors (see text).

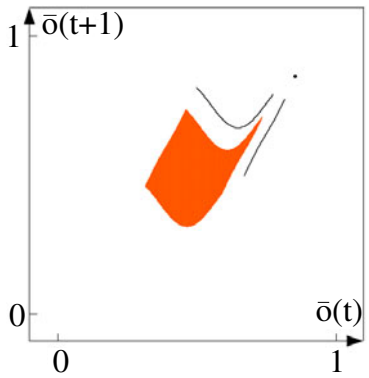

Figure 14. 3-chain 4.2: first return map of two chaotic attractors (grey area and the two lines) co-existing with one fixed point attractor for parameter values $-w_{21} = w_{23} = w_{12} = w_{32} = 8$, $\theta_1 = -3$, $\theta_2 = 5.65$, $\theta_3 = -7$. Plotted is the averaged output $\overline{o}$ of the module.

hysteresis interval with θ_2 increasing, only the reverse bifurcation sequence to the fixed point α is visible; crossing it with θ_2 decreasing, only the fixed point attractors γ appear. Although over the same interval there exists the additional bifurcation sequence ending in the period-2 attractors β, all its attractors stay invisible if one enters the θ_2-interval from outside. But they can be reached with θ_2 fixed in the hysteresis interval by choosing appropriate initial conditions. Two chaotic attractors co-existing with a fixed point attractor in this hysteresis domain for $\theta_2 = 5.65$ in figure 13 are shown in figure 14 in a pseudo-orbit representation (first return map), where $\overline{o}(t+1)$ is plotted against $\overline{o}(t)$, and $\overline{o}$ denotes the averaged module output $\overline{o} := \frac{1}{3}\sum_{i=1}^{3} o_i$. In figure 15 the projections of these attractors onto the three subspaces (o_1, o_2), (o_1, o_3), (o_2, o_3) are plotted: one of the chaotic attractors has the form of two straight lines, the other one comes as a rectangle; the fixed point is magnified. Parameters are again $-w_{21} = w_{23} = w_{12} = w_{32} = 8$, $\theta_1 = -3$, $\theta_2 = 5.65$, $\theta_3 = -7$. It is clearly seen from these projections that the attractors live on a two-dimensional sub-manifold.

Plotting the bifurcation sequences of figure 13 in both directions reveals even more domains of co-existing attractors. For instance, in the periodic window around $\theta_2 = 3.5$ one finds a period-3 attractor co-existing with a period-6 attractor. Both then are bifurcating with increasing θ_2 to higher-periodic attractors.

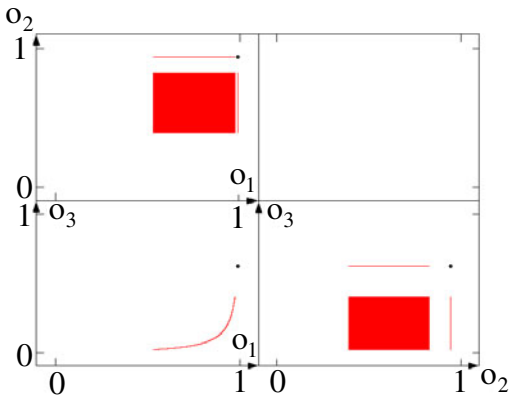

Figure 15. 3-chain 4.2: same attractors as in figure 14, but shown in terms of three projections of the output space (o_1, o_2, o_3).

4.3. Bi-directional 3-ring with one inhibitory neuron

The third candidate for complex dynamics is a 3-neuron module corresponding to a bi-directional ring (figure 8(*c*)). Its discrete dynamics is given by a nine-parameter family of maps $f_\rho : \boldsymbol{R}^3 \to \boldsymbol{R}^3$ defined by

$$\begin{aligned} a_1(t+1) &:= \theta_1 + w_{12}\,\sigma(a_2(t)) + w_{13}\,\sigma(a_3(t)), \\ a_2(t+1) &:= \theta_2 + w_{21}\,\sigma(a_1(t)) + w_{23}\,\sigma(a_3(t)), \\ a_3(t+1) &:= \theta_3 + w_{31}\,\sigma(a_1(t)) + w_{32}\,\sigma(a_2(t)). \end{aligned} \tag{28}$$

To expect complex dynamical behaviour for this module there should be an inhibitory neuron involved, e.g. neuron 1 with $w_{21}, w_{31} < 0$. The other neurons are chosen to be excitatory. Then the second and third rows of the linearization Df_ρ can satisfy condition (8) of our complex dynamics criterion. For neuron 3 we would get

$$w_{31}\sigma'(a_1) + w_{32}\sigma'(a_2) = 0. \tag{29}$$

The chaos condition (10) for the third component reads

$$\mathrm{Inv}_3 = w_{31}w_{13}\sigma'(a_1) + w_{23}w_{32}\sigma'(a_2) = 0,$$

which can be satisfied because in addition to $w_{31} < 0$ we have chosen $w_{13},\ w_{32},\ w_{23} > 0$.

The dynamics of this module, different to that of the other three-neuron modules discussed above, is in general three dimensional. Furthermore, due to lemma 1, the dynamics f_ρ (28) is again topologically conjugate to that of eight other parameter vectors $\rho' \in \boldsymbol{R}^9$ generated by the transformations T_k, $k = 1,\ 2,\ 3$ of equations (6) and (7). To get an impression of the dynamical complexity of this three-neuron module, we may take a look at the iso-periodic plot in the (θ_1, θ_2)-subspace in figure 16. Obviously we have to expect a complex dynamical behaviour again with co-existing attractors of different kind. This can be read from the overlapping regions in figure 16 around $\theta_1 = -4$, $\theta_2 = 1$. A bifurcation sequence in this domain will reveal further details, as, for instance, the one shown in figure 17. There we observe quasiperiodic attractors bifurcating from a fixed point attractor at around $\theta_1 = 0.46$. For a short interval these attractors co-exist with period-5 attractors (around $\theta_1 = 0$). With θ_1 further decreasing, a chaotic domain is entered which ends around $\theta_1 = -1.31$. Then a domain with period-2 attractors follows up to $\theta_1 = -4.88$, where a period-doubling route to chaos starts. Over the long interval $-5.77 < \theta_1 < -1.64$ together with the period-2 attractors there exist period-21 attractors.

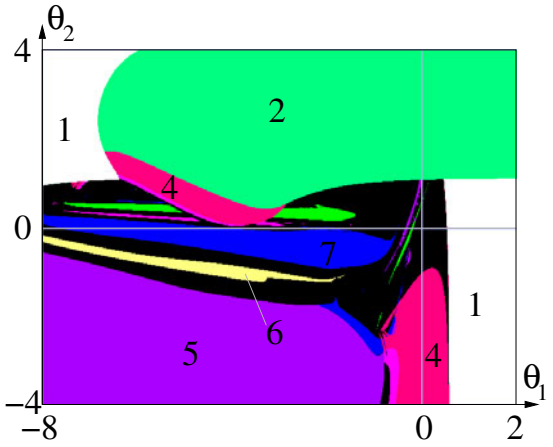

Figure 16. 3-ring 4.3: iso-periodic plot in the (θ_1, θ_2)-parameter subspace with fixed parameters $-w_{21} = -w_{31} = w_{23} = w_{12} = w_{32} = w_{13} = 8$, $\theta_3 = 5.5$. Numbers r refer to the existence of period-r attractors.

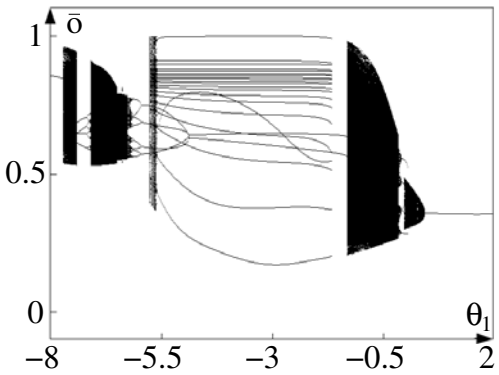

Figure 17. 3-ring 4.3: a bifurcation diagram for θ_1 with parameters $\theta_2 = 1$, $\theta_3 = 5.5$, $-w_{21} = -w_{31} = w_{23} = w_{12} = w_{32} = w_{13} = 8$ fixed. Plotted is the averaged output $\bar{o}$ of the module.

That the dynamics (28) is a genuine three-dimensional one can be seen in figure 18, where three projections of a chaotic attractor are shown. This attractor exists for parameter values $-w_{21} = -w_{31} = w_{23} = w_{12} = w_{32} = w_{13} = 8, \theta_1 = -1.75, \theta_2 = 0, \theta_3 = 5.5$.

4.4. Complex dynamics, no chaos

Finally we want to introduce two 3-neuron modules for which apparently no chaotic attractors exist, although there are higher-periodic attractors and interesting bifurcation sequences. The first example starts again with the bi-direction 3-ring (28), but with one weight equal to zero, for example $w_{23} = 0$. Then the complexity condition (29) for the third unit can still be satisfied but the chaos condition cannot be satisfied because it now reads

$$\mathrm{Inv}_1(a) = w_{31} w_{13} \sigma'(a_1) \sigma'(a_3) < 0, \qquad a \in \mathcal{A},$$

which is strictly negative.

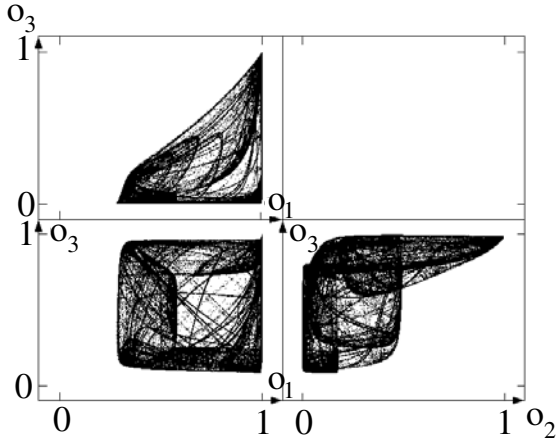

Figure 18. 3-ring 4.3: three projections of a chaotic attractor in the (o_1, o_2, o_3)-output space for parameter values $-w_{21} = -w_{31} = w_{23} = w_{12} = w_{32} = w_{13} = 8, \theta_1 = -1.75, \theta_2 = 0, \theta_3 = 5.5$.

The second example is given by an uni-directional 3-ring with one self-inhibitory neuron. Its dynamics is given by the equation

$$\begin{aligned} a_1(t+1) &:= \theta_1 + w_{11}\,\sigma(a_1(t)) + w_{13}\,\sigma(a_3(t)), \\ a_2(t+1) &:= \theta_2 + w_{21}\,\sigma(a_1(t)), \\ a_3(t+1) &:= \theta_3 + w_{32}\,\sigma(a_2(t)). \end{aligned} \tag{30}$$

The satisfiable complex dynamics condition (8) for the first component is given here by the equation

$$w_{11}\,\sigma'(a_1) + w_{13}\,\sigma'(a_3) = 0,$$

i.e. with $w_{11}w_{13} < 0$ and, for instance, $w_{11} < 0$. But the chaos condition cannot be satisfied because it reads

$$\mathrm{Inv}_1(a) = w_{11}^2(\sigma')^2(a_1) > 0, \qquad a \in \mathcal{A},$$

which is strictly positive.

5. Discussion

From the very simple example networks discussed in this paper there are some lessons to learn about artificial recurrent networks: first, from the point of view of dynamical systems theory, the sigmoidal transfer functions of neural networks provide an interesting nonlinearity for these systems. The simple chaotic 2-module already shows many dynamical effects, which are worth studying; i.e. there are period doubling routes to chaos, like in the quadratic map; there are Neimark–Sacker bifurcations from fixed point attractors to attractors with higher periods as well. All kinds of attractors can be observed: fixed points, higher periodic, quasi-periodic and chaotic attractors. Furthermore, for one and the same parameter vector attractors of different type can exist simultaneously, even different chaotic attractors.

This co-existence of attractors, often referred to as a multi-stability or multi-functionality property, gives rise to generalized hysteresis effects. Passing forward and backward over a hysteresis domain in parameter space makes the system switch between different attractors at different parameter values. As shown in figures 14 and 15, even dynamically non-trivial

attractors can co-exist, and the corresponding generalized hysteresis effect may serve as a kind of *short-term memory* of dynamical behaviours [45]. Much in the same way as the usual hysteresis effect serves as a memory of stationary states in magnets or computer chips. Thinking of attractors as representatives of mental or behaviour relevant states would explain, for instance, the flipping of the ambiguous figures in the visual domain or hysteresis effects in finger tapping [42] or bimanual coordination experiments [43].

It should be remarked that with respect to cognitive processes attractors will be always considered as representing a class of different dynamical solutions or trajectories. In fact, as part of cognitive systems the dynamics of neural networks will hardly ever be that of an attractor, because these systems are permanently driven by stimulating external sensor signals, or by internal stimuli coming from other parts of the cognitive system. Thus, what should be considered relevant for the discussion or interpretation of 'cognitive dynamics' are the basins of attraction of these systems; and properties of basin boundaries may be of more relevance for comprehending higher brain functions than the exact 'shape' of the representing attractors.

With respect to higher information processing or cognitive abilities (in the sense of non-trivial behaviour control) these dynamical neural networks represent a practically unlimited reservoir of possible behaviours. They can be coupled in very different ways, using excitatory as well as inhibitory connections between neurons of subsystems. Especially if recurrent couplings of such neuromodules are involved one can observe new or more 'complex' dynamical properties in the coupled system. This phenomenon of *emergent dynamics* is the basis for hopes that it will be possible to generate more powerful systems from specific coupling schemes of 'simple' neuromodules. At the same time, these nonlinear dynamical effects are a severe drawback for design or engineering approaches to such types of intelligent systems. This is because to date there is no theory which is able to predict the behaviour of coupled nonlinear systems; i.e. in a general setting one cannot predict analytically the number and types of attractors resulting from a given coupling, even if one knows the dynamical properties of the subsystems. Few results refer only to a very restricted class of neural networks and are mainly concerned with synchronization phenomena [22].

The abundance of dynamical phenomena in these neural reservoirs is overwhelming, and assuming complex dynamics to be the basis for the impressing abilities of biological brains suggests itself. There may even be chaos in the brain, as stated years ago by Skarda and Freeman [44], and having a closer look at biological brains, it would be very surprising *not* to find signals indicating chaotic dynamics in this very high-dimensional, highly connected recurrent network with inhibitory and excitatory path ways. But even if so, its functional role is still debatable and an open problem. The point we want to make in favour of chaotic neuromodules here is, that they provide the richest reservoir of possible dynamical features which are accessible by tuning the parameters correctly. If an input–output map must be realized: stationary states are available. If a specific periodic behaviour is necessary appropriate periodic attractors can be chosen. If chaotic dynamics is useful for representing 'emptiness', a resting state, or a specific function, it can be realized by the module. And 'drifting' parameters can switch between all these different modes. In this sense, chaotic modules are just powerful and versatile building blocks for systems which have to have a large reservoir of different behaviours at their disposal to adapt to an ever changing environment.

The choice of specific attractors or attractor combinations will, of course, be up to an adaptive self-organizing process on the parameter space of networks, which one may call *learning*. Learning is still a challenging problem for neural networks of general recurrent type. Thinking of these networks as controllers for the behaviour of biological or artificial

autonomous systems makes the problem even more challenging, because there is no way to determine the correct function of a subsystem during a goal-oriented behaviour. One way to get a deeper insight into the relation between structure and function of neuromodules, as well as into the effects of different types of couplings, is to study evolved neuro-controllers for autonomous agents. Examples for an evolutionary approach to behaviour-based robotics can be found, for instance, in [46] and [47].

References

[1] Abeles M 1991 *Corticonics* (Cambridge: Cambridge University Press)
[2] Arbib M A, Érdi P and Szentágothai J 1998 *Neural Organization—Structure, Function, and Dynamics* (Cambridge, MA: MIT Press)
[3] Shepherd G M (ed) 1990 *The Synaptic Organization of the Brain Cortex* (New York: Oxford University Press)
[4] White E L 1989 *Cortical Circuits: Synaptic Organization of the Cerebral Cortex Structure, Function and Theory* (Boston, MA: Birkhäuser)
[5] Szentagothai J 1983 The modular architectonic principle of neural centers *Rev. Physiol. Biochem. Pharmacol.* **98** 11–61
[6] Mackey M C, and an der Heiden U 1984 The dynamics of recurrent inhibition *J. Math. Biol.* **19** 211–25
[7] Traub R D and Miles R 1991 *Neuronal Networks of the Hippocampus* (New York: Cambridge University Press)
[8] Wilson H R and Cowan J D 1972 Excitatory and inhibitory interactions in localized populations of model neurons *Biophys. J.* **12** 1–23
[9] Douglas R J, Martin K A C and Whitteridge D 1989 A canonical microcircuit for neocortex *Neural Comput.* **1** 480–88
[10] Buzsáki G, Llinás R, Singer W, Berthoz A and Christen Y (ed) 1994 *Temporal Coding in the Brain* (Berlin: Springer)
[11] Duke W and Pritchard W S (ed) 1991 *Proc. Conf. on Measuring Chaos in the Human Brain* (Singapore: World Scientific)
[12] Elbert T, Ray W J, Kowalik Z J, Skinner J E, Graf K E and Birbaumer N 1994 Chaos and physiology: deterministic chaos in excitable cell assemblies *Physiol. Rev. Am. Physiol. Soc.* **74** 1–47
[13] Pantev C, Elbert T and Lutkenhöhner B (ed) 1995 *Oscillatory Event-Related Brain Dynamics* (London: Plenum)
[14] An der Heiden U 1980 *Analysis of Neural Networks (Lecture Notes in Biomathematics vol 35)* (Berlin: Springer)
[15] Marcus C M and Westervelt R M 1989 Dynamics of iterated-map neural networks *Phys. Rev.* A **40** 501–4
[16] Renals S and Rohwer R 1990 A study of network dynamics *J. Stat. Phys.***58** 825–48
[17] Wang X 1991 Period-doublings to chaos in a simple neural network: an analytic proof *Complex Syst.* **5** 425–41
[18] Blum E K and Wang X 1992 Stability of fixed points and periodic orbits and bifurcations in analog neural networks *Neural Netw.* **5** 577–87
[19] Chapeau-Blondeau F and Chauvet G 1992 Stable, oscillatory, and chaotic regimes in the dynamics of small neural networks with delay *Neural Netw.* **5** 735–43
[20] Borisyuk R M and Kirillov A 1992 Bifurcation analysis of neural network model *Biol. Cybern.* **66** 319–25
[21] Beer R D 1995 On the dynamics of small continuou-time recurrent networks *Adapt. Behav.* **3** 471–511
[22] Tonnelier A, Meignen S, Bosch H and Demongeot J 1999 Synchronization and desynchronization of neural oscillators *Neural Netw.* **12** 1213–28
[23] Piñeiro J D, Marichal R L, Moreno L, Sigut J F and González E J 2001 Study of chaos in a simple discrete recurrence Neural Network *Bio-Inspired Applications of Connectionism. Proc. IWANN'2001 (LNCS vol 2085)* ed J Mira and A Prieto (Berlin: Springer) pp 579–85
[24] Pasemann F 1995 Neuromodules: a dynamical systems approach to brain modelling *Supercomputing in Brain Research—From Tomography to Neural Networks* ed H Herrmann, E Pöppel and D Wolf (Singapore: World Scientific) pp 331–47
[25] Pasemann F 1998 Structure and dynamics of recurrent neuromodules *Theor. Biosci.* **117** 1–17
[26] Pakdaman K, Grotta-Ragazzo C, Malta C P, Arino O and Vibert J F 1998 Effect of delay on the boundary of the basins of attraction in a system of two neurons *Neural Netw.* **11** 509–19
[27] Botelho F 1999 Dynamical features simulated bby recurrent neural networks *Neural Netw.* **12** 609–15
[28] Klotz A and Brauer K 1999 A small-size neural network for computing with strange attractors *Neural Netw.* **12** 601–7
[29] Schwarz J, Klotz A, Bräuer K and Stevens A 2001 Master-slave synchronization in chaotic discrete-time oscillators *Phys. Rev.* E **64** 11 108–17

[30] Tino P, Horne B G and Giles C L 2001 Attractive periodic sets in discrete time recurrent networks *Neural Comput.* **13** 1379–414
[31] Thom R 1975 *Structural Stability and Morphogenesis* (Reading, MA: Benjamin)
[32] Poston T and Stewart I 1978 *Catastrophe Theory and its Applications* (London: Pitman)
[33] Pasemann F 1993 Dynamics of a single model neuron *Int. J. Bifur. Chaos* **2** 271–8
[34] Port R and van Gelder T (ed) 1995 *Mind as Motion: Explorations in the Dynamics of Cognition* (Cambridge, MA: MIT Press)
[35] Herz A V M 1996 Global analysis of recurrent neural networks *Models of Neural Networks* vol 3, ed E Domany, J L van Hemmen and K Schulten (New York: Springer)
[36] Martelli M 1999 *Introduction to Discrete Dynamical Systems and Chaos* (New York: Wiley)
[37] Kaszkurewicz E and Bhaya A 2000 *Matrix Diagonal Stability in Systems and Computation* (Boston, MA: Birkhäuser)
[38] Pasemann F 1995 Characteristics of periodic attractors in neural ring networks *Neural Netw.* **8** 421–9
[39] Thompson J M T and Stewart H B 1986 *Nonlinear Dynamics and Chaos* (Chichester: Wiley)
[40] Abraham R H, Gardini L and Mira C 1997 *Chaos in Discrete Dynamical Systems* (New York: Springer)
[41] Pasemann F and Wennekers T 2000 Generalized and partial synchronization of coupled neural networks *Network: Comput. Neural Syst.* **11** 41–61
[42] Kelso J A S, DelColle J D and Schöner G 1990 Action-perception as a pattern formation process *Attention and Performance* vol 13, ed M Jeannerod (Hillsdale, NJ: Erlbaum) pp 139–69
[43] Kelso J A S 1995 *Dynamic Patterns—The Self-Organization of Brain and Behavior* (Cambridge, MA: MIT Press)
[44] Skarda C A and Freeman W J 1987 How brains make chaos in order to make sense of the world? *Behav. Brain Sci.* **10** 161–95
[45] Foss J, Moss F and Milton J 1997 Noise, multistability and delayed recurrent loops *Phys. Rev.* E **55** 4536–43
[46] Pasemann F, Steinmetz U and Hülse M 2001 Robot control and the evolution of modular neurodynamics *Theor. Biosci.* **120** 311–26
[47] Nolfi S and Floreano D 2000 *Evolutionary Robotics: The Biology, Intelligence, and Technology of Self-Organizing Machines* (Cambridge, MA: MIT Press)